

Single vibronic level emission spectroscopy of the $\tilde{A}^1B_1 \rightarrow \tilde{X}^1A_1$ system of dibromocarbene

Chong Tao, Calvin Mukarakate, Scott A. Reid *

Department of Chemistry, Marquette University, Milwaukee, WI 53201-1881, USA

Received 30 October 2006; in revised form 28 November 2006

Available online 2 December 2006

Abstract

Following the development of an improved discharge recipe for production of dibromocarbene (CBr_2), and an extensive spectroscopic survey of the $\tilde{A}^1B_1 \leftarrow \tilde{X}^1A_1$ system that has led to a revision in the position of the origin, we have recorded single vibronic level (SVL) emission spectra of $\text{C}^{79}\text{Br}^{81}\text{Br}$ and C^{81}Br_2 which probe the vibrational structure of the \tilde{X}^1A_1 state up to $\sim 7000 \text{ cm}^{-1}$ above the vibrationless level. These spectra reveal many previously unassigned levels. In the region between ~ 3600 and 5900 cm^{-1} , or between the singlet–triplet gap proposed by Hsu et al. [H.-J. Hsu, W.-Z. Chang, B.-C. Chang, Phys. Chem. Chem. Phys. 2005, 7, 2468–2473] to that predicted by theory, we find that $\sim 90\%$ of the lines can be assigned to \tilde{X}^1A_1 levels within three standard deviations of our Dunham expansion fit, suggesting that the vast majority of emission lines terminate on levels of the singlet state. A nearly complete set of vibrational parameters was determined for the \tilde{X}^1A_1 state; the derived parameters are in good agreement with recent *ab initio* predictions. © 2006 Elsevier Inc. All rights reserved.

Keywords: Carbenes; Electronic spectroscopy; Renner–Teller effect; Spin–orbit coupling; Singlet–triplet gap

1. Introduction

Carbenes are important reactive intermediates in many chemical processes [1–6]. These species contain a divalent carbon, giving rise to singlet and triplet configurations of similar energy but very different reactivity. Thus, the magnitude of the singlet–triplet gap (ΔE_{ST}) is an important quantity needed to predict the reactivity of carbenes in environments where both states can be populated. The mono- and dihalocarbenes have served as important test cases for comparing experimental and theoretically derived ΔE_{ST} 's, and recent progress has been made in determining ΔE_{ST} for a number of carbenes [7–22]. For example, in CHCl the experimental value for $T_{00}(\tilde{a} - \tilde{X})$ of $2172(2) \text{ cm}^{-1}$, derived via single vibronic level emission spectroscopy [17,21], is within 2 cm^{-1} of a theoretical estimate at the CCSD(T)/aug-cc-pVQZ level which included

relativistic, core correlation and diagonal Born–Oppenheimer corrections [19].

Of all carbenes, the magnitude of the singlet triplet gap is perhaps most controversial for the dihalocarbenes CCl_2 and CBr_2 . For CCl_2 , calculations predict a singlet ground state with $\Delta E_{\text{ST}} \sim 20 \text{ kcal mol}^{-1}$ ($\sim 7000 \text{ cm}^{-1}$) [19,23–45], and a recent CCSD(T)/aug-cc-pVQZ calculation which included relativistic, core correlation and diagonal Born–Oppenheimer corrections located the gap at 7050 cm^{-1} [19]. For CBr_2 , calculations also predict a singlet ground state with $\Delta E_{\text{ST}} \sim 17 \text{ kcal mol}^{-1}$ ($\sim 5900 \text{ cm}^{-1}$) [30–32,34,35,38–40,42,44,46,47]. These results lie in stark contrast to the photoelectron studies of CCl_2^- and CBr_2^- by Lineberger and co-workers [7,9], which place the gap at $3(\pm 3) \text{ kcal mol}^{-1}$ for CCl_2 and $2(\pm 3) \text{ kcal mol}^{-1}$ for CBr_2 [9]. Recently, it has been suggested that the photoelectron spectra may contain contributions from a quartet state of the anion, which might explain this discrepancy [44,45].

A successful approach to determining ΔE_{ST} for the monohalocarbenes CHCl and CHBr is single vibronic level emission spectroscopy [10–12,14,15,17,18,20–22], and this

* Corresponding author. Fax: +1 414 288 7660.
E-mail address: scott.reid@mu.edu (S.A. Reid).

technique has recently been extended to the dihalocarbenes [15,16,48,49]. Miller, Chang and co-workers obtained emission spectra of CCl_2 which probed the vibrational structure of the \tilde{X}^1A_1 state [16], and reported unassigned structure beginning $\sim 5000\text{ cm}^{-1}$ ($\sim 14\text{ kcal mol}^{-1}$) above the \tilde{X}^1A_1 origin which they attributed to levels of the \tilde{a}^3B_1 state. In a recent study [49], we tested for the presence of \tilde{a}^3B_1 levels in the high energy region of the CCl_2 emission spectrum using K'_a -sorted emission spectra; these discriminate between singlet and triplet levels via the $(A'' - \bar{B}'')$ rotational constant, which is significantly larger for pure triplet levels due to the larger equilibrium bond angle of the triplet state. In the region between ~ 3500 and 9000 cm^{-1} above the vibrationless level of the \tilde{X}^1A_1 state, we found only a very modest increase in $(A'' - \bar{B}'')$, and $\sim 86\%$ of the lines observed between 5000 and 9000 cm^{-1} could be assigned to \tilde{X}^1A_1 levels within 3 standard deviations of our Dunham expansion fit, which included more than 140 levels in total.

Recently, Hsu et al. [48] recorded SVL emission spectra of CBr_2 . Due to extensive interference from HBr and Br_2 , emission spectra were only obtained for two bands, 2_0^{12} and 2_0^{13} (labels follow our revised assignment of the electronic origin) [50]. These authors reported that the pure bending progression $(0, n, 0)$ did not appear in their emission spectrum, which is surprising given that: (1) this progression appears in the emission spectrum of every other triatomic carbene [16,20,21,49], (2) it was reported in the initial matrix emission studies of CBr_2 [51,52], and (3) a long bending progression is observed in the excitation spectrum of CBr_2 [53–55]. In addition, they reported congested, unassigned structure beginning $\sim 3650\text{ cm}^{-1}$ above the \tilde{X}^1A_1 origin which was attributed to levels of the \tilde{a}^3B_1 state, leading to an estimated ΔE_{ST} of $10.4\text{ kcal mol}^{-1}$. However, this assignment is problematic in at least two respects. First, as the observation of spin–orbit perturbations does not necessarily coincide with the position of the triplet origin, the discrepancy with theory is uncomfortably large (i.e., $>6\text{ kcal mol}^{-1}$ or 2200 cm^{-1}). To explain this, the authors invoke a large spin–orbit matrix element; however, in the related monohalocarbene CHBr the derived matrix elements are on the order of $\sim 330\text{ cm}^{-1}$ [13,22]. Second, the observed \tilde{X}^1A_1 state vibrational term energies up to $\sim 5200\text{ cm}^{-1}$ were fit to a Dunham expansion with a standard deviation of $\sim 2.3\text{ cm}^{-1}$ [48], i.e., within the experimental uncertainty, which suggests a lack of spin–orbit perturbations in this region. Note that a similar fit for CHBr , where ΔE_{ST} is much lower, returns a standard deviation of $\sim 16\text{ cm}^{-1}$ due to extensive spin–orbit mixing [20].

In this study, we report extensive single vibronic level (SVL) emission spectra of CBr_2 , obtained following the development of an improved discharge recipe for production of this carbene free from interference of CHBr or Br_2 [50]. We have recorded and rotationally analyzed the complete visible fluorescence excitation spectrum of CBr_2 , leading to a revision in the assignment of the electronic origin of this system [50]. For this work, we recorded emission spectra for both C^{81}Br_2 and $\text{C}^{79}\text{Br}^{81}\text{Br}$ isotopomers from a

variety of \tilde{A}^1B_1 state levels. These reveal the pure bending progression, and we show that the congested structure noted by Hsu et al. [48] reflects the near 3:1 resonance between the ground state symmetric stretching and bending frequencies. In the region between ~ 3500 and 5800 cm^{-1} above the vibrationless level of the \tilde{X}^1A_1 state, or from the singlet–triplet gap proposed by Hsu et al. [48] to that predicted by theory, we find that $\sim 90\%$ of the observed lines can be assigned to \tilde{X}^1A_1 levels within 3 standard deviations of our Dunham expansion fit, which included almost 100 levels in total. A nearly complete set of vibrational parameters was determined for the $\text{C}^{79}\text{Br}^{81}\text{Br}$ and $\text{C}^{81}\text{Br}^{81}\text{Br}$ isotopomers, and these are compared with theoretical predictions.

2. Experimental section

The apparatus, pulsed discharge nozzle, and data acquisition procedures have been described in detail in recent studies [20–22]. In previous discharge studies [15,48], the carbene CBr_2 was produced using a pulsed electrical discharge through a mixture of CBr_4 and CHBr_3 seeded in high purity He. These spectra suffered from large CHBr and Br_2 impurity signals [48]; note that several of the peaks assigned to Br_2 in this work are actually transitions of CHBr [20]. In our previous CHBr studies [20], we found that CHBr fluorescence was almost entirely suppressed when using Ar as carrier gas. Thus, in the present study we passed Ar gas at a pressure of 2–3 bar over a solution containing CBr_4 in CHBr_3 held in a stainless steel bubbler at room temperature. The discharge was initiated by a +1 kV pulse of $\sim 90\text{ }\mu\text{s}$ duration, through a current limiting $10\text{ k}\Omega$ ballast resistor. As demonstrated below, these conditions produced strong CBr_2 fluorescence signals nearly free of CHBr and Br_2 impurities.

The timing of laser, nozzle, and discharge firing was controlled by a digital delay generator (Stanford Research Systems DG535), which generated a variable width gate pulse for the high voltage pulser (Directed Energy GRX-1.5K-E). The laser system consisted of an etalon narrowed dye laser (Lambda-Physik Scanmate 2E) pumped by the second or third harmonic (532 or 355 nm) of a Nd:YAG laser (Continuum NY-61). The laser beam was not focused, and typical pulse energies were ~ 1 to 2 mJ in a $\sim 3\text{ mm}$ diameter beam. A mutually orthogonal geometry of laser, molecular beam, and detector was used, where the laser beam crossed the molecular beam at a distance of $\sim 1\text{ cm}$ downstream. Fluorescence was collected and collimated by a 2 in. diameter, $f/2.4$ plano-convex lens, and focused into the spectrograph using a f -matching $f/3.0$ plano-convex lens, also 2 in. in diameter. Insertion of an aluminum mirror into the beam path at 45° allowed collection of the total fluorescence, which was filtered via an appropriate long-pass cutoff filter (Corion or Edmund Scientific) prior to striking a photomultiplier tube detector (Oriel) held at typically -700 V . In acquiring emission spectra, the fluorescence signal was first optimized on the band of interest,

and the mirror subsequently removed to allow fluorescence to enter the spectrograph. A second removable mirror assembly was used to direct the output of an Fe:Ne hollow cathode lamp into the spectrograph for wavelength calibration; these spectra were typically obtained immediately after the emission spectra. Background spectra were obtained with the laser blocked to check for emission lines from species in the discharge.

The spectrograph used in this work was an Acton SR303i equipped with an ISTAR intensified CCD camera. Calibration spectra were acquired with a slit width of 10 μm and 500 shot accumulation; photon counting was not used. The emission spectra were acquired in photon counting mode (10,000 shot typical accumulation) with a slit width of 50–100 μm , using a 600 lines/mm grating blazed at 500 nm. The integration gate (typically 8 μs) was set to fully encompass the fluorescence decay of the emitting level under our experimental conditions, and the spectrograph was operated in a “step and glue” mode, where the grating was sequentially stepped and spectra recorded at each grating position in order to cover the entire spectral region of interest. Spectra were calibrated in each range by first fitting the Ne I emission lines to a Gaussian lineshape function, using Origin 7.5 software. The observed positions were then compared against the known values [56], and the deviations fit to a second order polynomial to obtain a calibration curve which was applied to the corresponding emission spectrum. Bands in the emission spectra were also fit to a Gaussian lineshape function.

3. Results and discussion

The fluorescence excitation spectrum of the $\tilde{A}^1B_1 \leftarrow \tilde{X}^1A_1$ system of CBr_2 was first obtained in an Ar matrix by Bondebey et al., who assigned the origin to a band at 14 962 cm^{-1} [53]. Later, Zhou et al., measured the room temperature gas-phase spectrum and assigned the origin to 14 885 cm^{-1} [54]. In 1993, Xu and Harmony reported a detailed analysis of the spectrum under jet-cooled conditions using a pyrolysis source [55], and argued based upon the observed isotope shifts that the vibrational assignments of Zhou et al., were off by one quantum; the origin was therefore reassigned to $\sim 15\,192\text{ cm}^{-1}$. Recently, we have shown from an improved analysis of the excited state isotope shifts that both previous gas phase assignments are incorrect [50]; we reassigned the origin to $\sim 15\,297\text{ cm}^{-1}$, in good agreement with recent *ab initio* predictions [40,57].

Our rotational analysis of bands in the $\tilde{A}^1B_1 \leftarrow \tilde{X}^1A_1$ system show that the isotope splittings increase linearly with energy, so that bands of the various isotopomers are relatively well separated in the high energy region of the spectrum. For this study, we chose bands where isotope and K'_a selectivity was possible for the C^{81}Br_2 and $\text{C}^{79}\text{Br}^{81}\text{Br}$ isotopomers, and emission spectra were therefore obtained only after rotational simulation of the excitation spectra. An example experimental and simulated spectrum for the $1_0^2 2_0^9$ band is shown in Fig. 1, together with individual simulations for

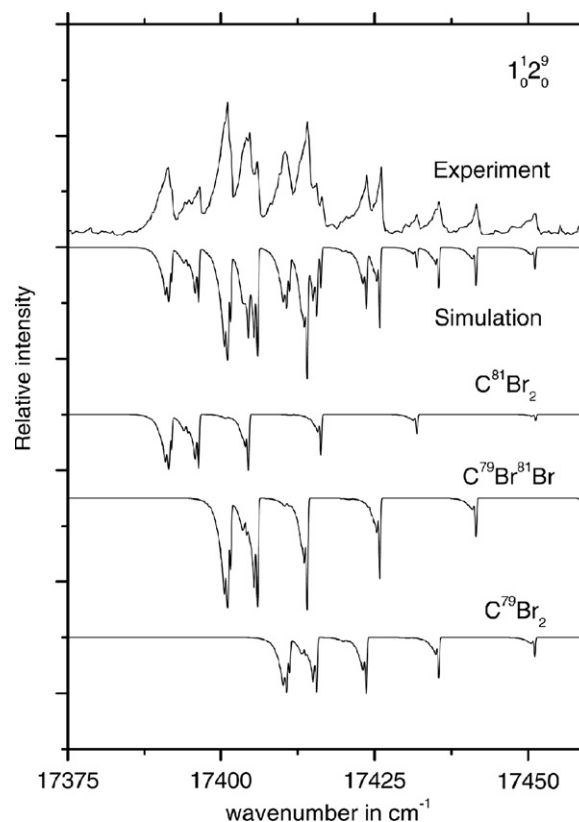


Fig. 1. Experimental (upper) and simulated fluorescence excitation spectrum of the $1_0^2 2_0^9$ band in the $\tilde{A}^1B_1 \leftarrow \tilde{X}^1A_1$ system of CBr_2 .

the three isotopomers. The simulations were scaled to reflect the 1:2:1 isotopomer ratio, and the total (summed) spectrum scaled to match the experiment. Note that the full results of our rotational analysis of bands in the $\tilde{A}^1B_1 \leftarrow \tilde{X}^1A_1$ system will be reported in a future publication.

Fig. 2 displays example SVL emission spectra of the $\text{C}^{79}\text{Br}^{81}\text{Br}$ isotopomer obtained by pumping the $K'_a = 0$ level of the $1_0^2 2_0^9$ and 2_0^9 bands. These spectra show a good signal-to-noise ratio, and reveal structure extending up to $\sim 7000\text{ cm}^{-1}$ above the \tilde{X}^1A_1 state origin. We obtained SVL emission spectra of the $\text{C}^{79}\text{Br}^{81}\text{Br}$ isotopomer from the \tilde{A} state levels $1^2 2^9$, 2^9 , 2^{12} , 2^{15} , and $1^1 2^{15}$, and spectra of the C^{81}Br_2 isotopomer from the \tilde{A} state levels $1^2 2^7$, $1^1 2^{12}$, 2^{12} , $1^1 2^{15}$, and 2^{15} . By using a variety of pump transitions, we exploit variations in Franck–Condon factors to observe the maximum possible number of \tilde{X} state levels and eliminate spurious peaks due to the discharge background or collision-induced relaxation in the \tilde{A} state. The derived \tilde{X} state term energies of the $\text{C}^{79}\text{Br}^{81}\text{Br}$ isotopomer are compared in Table 1 with previous work from Chang and co-workers [48]. At low energies (i.e., $< 3000\text{ cm}^{-1}$) the agreement is good; at higher energies some large deviations are observed. We have assigned many more lines in the high energy region of the spectrum.

We fit the observed term energies using a nonlinear least squares routine to a standard anharmonic potential function (Dunham expansion) of the form [58]:

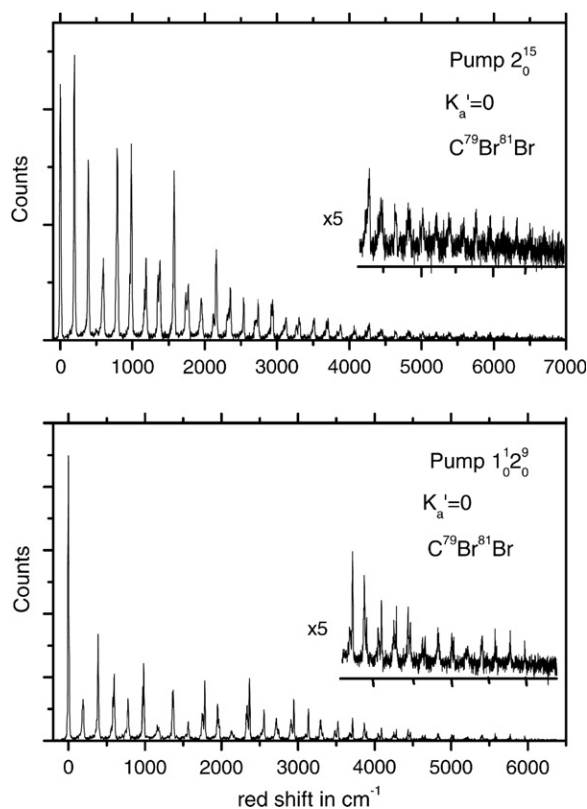


Fig. 2. Single vibronic level emission spectra of $C^{79}Br^{81}Br$ from the $K'_a = 0$ level of the 2^{15} (upper) and 1^{129} bands (labels follow our revised assignment [Ref. 50]). In each panel expanded (5 \times) views of the high energy region are shown.

$$G(v_1, v_2, v_3) = \sum_{i=1}^3 (v_i + 1/2)\omega_i + \sum_{j \geq i, i=1}^3 (v_i + 1/2)(v_j + 1/2)x_{ij}, \quad (1)$$

where ω_i is the harmonic frequency of mode i , x_{ii} is a diagonal anharmonicity constant, and x_{ij} is an off-diagonal or cross-anharmonicity constant. The parameter x_{33} could not be determined and was fixed at 0.0 cm^{-1} in the fit; the derived frequency for v_3 is thus an anharmonic frequency. The fit to 92 levels of the $C^{79}Br^{81}Br$ isotopomer returned a standard deviation of 2.7 cm^{-1} , within our experimental uncertainty of $\sim 4 \text{ cm}^{-1}$. The Dunham parameters are given in Table 2, along with theoretical predictions of the harmonic vibrational frequencies; [40] the agreement is very good. The corresponding term energies and Dunham parameters for the $C^{81}Br_2$ isotopomer are provided in the supporting information. When high resolution rotational information becomes available, this data will be useful in deriving a harmonic force field for the ground state.

Focusing on the $3650\text{--}5900 \text{ cm}^{-1}$ region, or from the singlet-triplet gap proposed by Hsu et al. [48] to the calculated singlet-triplet gap, we observe a total of 51 lines for the $C^{79}Br^{81}Br$ isotopomer which we are confident belong to unrelaxed SVL emission. Of these, 46 (90%) can be

Table 1
Vibrational term energies (in cm^{-1}) for the \tilde{X}^1A_1 state of $C^{79}Br^{81}Br$ derived from SVL emission spectra

Level	Term energy ^a		o. - c. ^b
	This work	Ref. [48]	
(0,1,0)	192(3)	...	-3
(0,2,0)	386(4)	...	0
(0,3,0)	579(4)	...	4
(1,0,0)	597(2)	599	0
(0,4,0)	764(13)	...	3
(1,1,0)	786(6)	792	-4
(1,2,0)	982(5)	976	1
(0,6,0)	1122(6)	...	-1
(1,3,0)	1165(6)	1170	-3
(2,0,0)	1189(3)	1187	-1
(0,0,2)	1349(6)	...	3
(1,4,0)	1349(6)	1357	-3
(2,1,0)	1378(3)	1382	-3
(1,5,0)	1534(5)	...	0
(0,1,2)	1534(5)	...	-2
(2,2,0)	1570(5)	1569	0
(2,3,0)	1759(4)	1758	2
(3,0,0)	1777(6)	1774	-1
(1,0,2)	1926(5)	...	5
(2,4,0)	1940(2)	1943	-1
(3,1,0)	1968(2)	1967	-1
(0,4,2)	2081(10)	...	-5
(1,1,2)	2106(2)	...	-4
(2,5,0)	2122(4)	2133	2
(0,12,0)	2140(6)	...	1
(3,2,0)	2162(3)	2159	5
(3,3,0)	2342(2)	2347	0
(4,0,0)	2362(5)	2347	-1
(1,3,2)	2480(5)	...	2
(3,4,0)	2523(8)	...	-2
(4,1,0)	2554(5)	2547	2
(3,5,0)	2705(6)	...	2
(1,12,0)	2718(2)	...	-3
(4,2,0)	2744(4)	2742	5
(0,17,0)	2903(3)	...	0
(4,3,0)	2919(9)	2928	-4
(5,0,0)	2943(3)	2928	0
(3,0,2)	3060(3)	...	-1
(4,4,0)	3103(6)	...	-2
(5,1,0)	3130(6)	...	-2
(3,1,2)	3246(7)	...	0
(0,11,2)	3267(2)	...	1
(4,5,0)	3280(8)	...	-2
(2,12,0)	3299(6)	...	1
(5,2,0)	3322(6)	3312	4
(2,13,0)	3452(5)	...	-3
(4,6,0)	3452(5)	...	-5
(1,17,0)	3481(5)	...	2
(5,3,0)	3503(6)	3508	3
(6,0,0)	3516(3)	3496	-4
(2,14,0)	3608(3)	...	-1
(3,3,2)	3608(3)	...	-1
(5,4,0)	3681(4)	...	2
(6,1,0)	3709(2)	3691	2
(3,12,0)	3867(4)	...	-5
(6,2,0)	3893(6)	3885	2
(2,17,0)	4054(4)	...	3
(7,0,0)	4091(2)	4066	-1
(5,7,0)	4200(7)	...	0
(2,10,2)	4228(2)	...	-1

(continued on next page)

Table 1 (continued)

Level	Term energy ^a		o. – c. ^b
	This work	Ref. [48]	
(6,4,0)	4252(3)	...	1
(7,1,0)	4279(4)	4262	1
(5,8,0)	4369(5)	...	2
(4,12,0)	4437(2)	...	-6
(7,2,0)	4464(2)	4450	3
(2,20,0)	4464(2)	...	-3
(4,13,0)	4597(2)	...	1
(6,6,0)	4597(2)	...	-1
(3,9,2)	4626(3)	...	1
(7,3,0)	4638(3)	4645	-4
(8,0,0)	4657(2)	4626	-3
(3,10,2)	4784(6)	...	0
(7,4,0)	4818(4)	...	-1
(8,1,0)	4841(4)	4823	-4
(7,5,0)	4998(4)	...	6
(5,12,0)	5008(2)	...	-1
(8,2,0)	5030(3)	5014	3
(7,6,0)	5164(2)	...	0
(4,9,2)	5176(4)	...	-1
(8,3,0)	5208(4)	5204	2
(8,4,0)	5384(4)	...	2
(9,1,0)	5406(6)	...	-3
(8,5,0)	5554(2)	...	0
(6,12,0)	5571(5)	...	1
(9,2,0)	5590(3)	...	1
(6,13,0)	5722(3)	...	1
(8,6,0)	5722(3)	...	-3
(9,3,0)	5771(2)	...	4
(9,4,0)	5941(2)	...	-1
(7,12,0)	6126(5)	...	-2
(10,3,0)	6319(8)	...	-4

Assignments and deviations from a Dunham expansion fit are given.

^a One standard error given in parenthesis (right justified).

^b Observed – calculated.

Table 2
C⁷⁹Br⁸¹Br vibrational parameters determined from the Dunham expansion fit, compared with theoretical predictions

Parameter	Dunham fit (this work)	Ab initio (Ref. [39])
ω_1	606.6(4)	601.6
ω_2	199.5(2)	196.6
ν_3	679.8(7)	655.3
x_{11}	-2.01(4)	...
x_{12}	-1.23(2)	...
x_{13}	-10.66(29)	...
x_{22}	-1.49(1)	...
x_{23}	-2.60(10)	...
x_{33}	0.0 ^a	...

^a Fixed in the fit.

assigned to singlet lines in the $(n,m,0)$ and $(n,m,2)$ progressions (n,m represent integers ≥ 0) within three standard deviations of the Dunham fit. Thus, while there are a few unassigned lines in this region, the vast majority of emission lines terminate on levels of the singlet state. We suggest that the congested structure in this region does not arise from spin-orbit interactions but rather reflects the near 3:1 resonance of the ground state symmetric stretching

and bending frequencies, which produces a polyad structure, with levels in a given polyad characterized by the polyad quantum number $p = 3n + m$. For example, the $p = 6$ polyad consists of three levels: $(2,0,0)$ at 1187 cm^{-1} , $(1,3,0)$ at 1165 cm^{-1} , and $(0,6,0)$ at 1122 cm^{-1} , as shown in Fig. 3. As is evident from Fig. 2, this polyad structure continues to high energy (we have measured up to $p = 34$), with the intrapolyad spacing increasing somewhat with energy. Due, however, to the fact that only a few levels in each polyad display significant Franck-Condon activity, the spectrum retains a regular appearance. As evidenced from the quality of our Dunham fit, the levels within a given polyad do not strongly interact.

To probe for triplet levels in the high energy region of the spectrum, we used K_a -sorted emission spectroscopy [49], a method previously used by us to probe for the presence of triplet levels in CHCl and C³⁵Cl₂. This method takes advantage of the large ($\sim 20^\circ$) increase in equilibrium bond angle for the triplet state, which leads to a larger A rotational constant for triplet levels. In beginning this work, we anticipated that CBr₂ would be an ideal system for application of this method; however, the polyad structure in the spectrum leads to few (if any) isolated lines in the high energy region of the spectrum. Fig. 4 shows expanded views of the $4700\text{--}6600 \text{ cm}^{-1}$ region (i.e., centered on the theoretical position of the triplet origin) for spectra obtained by pumping $K'_a = 0$ and 2 for the C⁷⁹Br⁸¹Br isotopomer in the 2_0^{15} band. From the

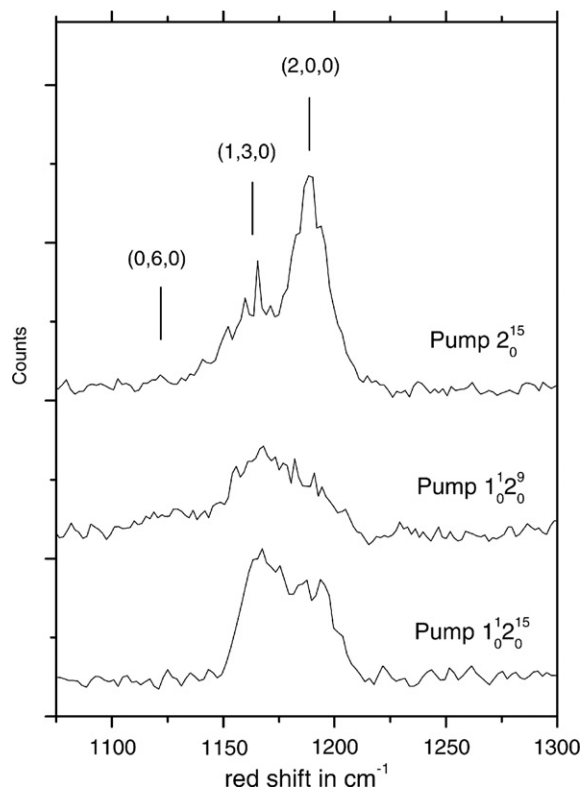


Fig. 3. Expanded single vibronic level emission spectra of C⁷⁹Br⁸¹Br in the region of the $p = 6$ polyad obtained by pumping the 2_0^{15} , $1_0^2_9$, and $1_0^2_{15}$ bands.

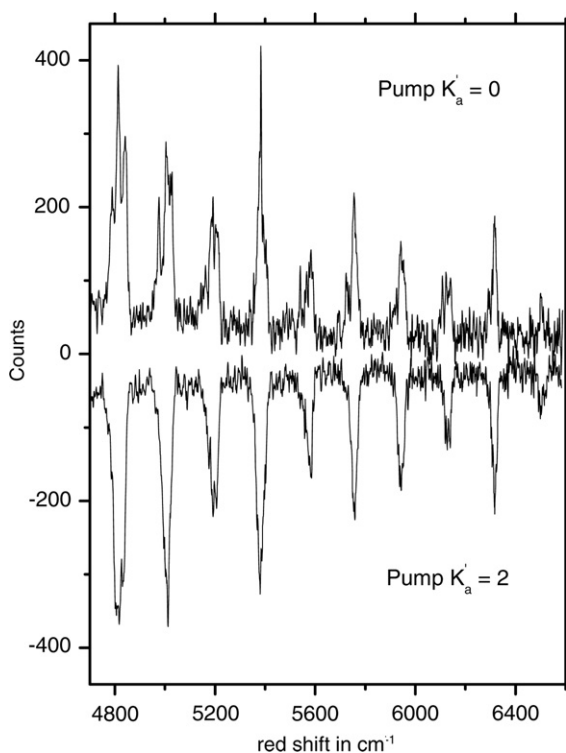


Fig. 4. Expanded and K_a -sorted single vibronic level emission spectra of $C^{79}Br^{81}Br$ in the region of the predicted triplet origin. Spectra were obtained by pumping the $K'_a = 0$ (upper) and $K'_a = 2$ levels of the 2^{15} band.

$\Delta K_a = \pm 1$ selection rule, levels in the $K'_a = 0$ spectra are not split, while those in the $K'_a = 2$ spectra are split by $8(A'' - \bar{B}'')$ [49], the calculated rotational constants for the vibrationless levels of the \tilde{X}^1A_1 and \tilde{a}^3B_1 states [40] suggest splittings of ~ 10 and 19 cm^{-1} , respectively, for pure (unmixed) singlet and triplet levels. However, due to the spectral congestion, we were unable to determine the $(A'' - \bar{B}'')$ constants in this region; the 4800 cm^{-1} polyad ($p = 25$) illustrates the problem. The $K'_a = 0$ spectrum (Fig. 4) shows at least three transitions: (3,10,2) at 4784 cm^{-1} , (7,4,0) at 4818 cm^{-1} , and (8,1,0) at 4841 cm^{-1} . In the $K'_a = 2$ spectrum, these lines begin to split, and the spectrum is broadened. Due to degree of overlap, the splittings, and thus $(A'' - \bar{B}'')$ constants, cannot be accurately determined, even from spectra measured for higher K'_a . Thus, it is clear that higher resolution studies (using, e.g., stimulated emission pumping (SEP) spectroscopy) will be needed to probe for the presence of triplet lines in this region. This work has set the stage for such experiments by reporting many new lines in the high energy region of the spectrum and an extensive set of vibrational constants for the ground state.

4. Conclusions

Following the development of an improved discharge recipe for production of CBr_2 , and an extensive spectroscopic survey of the $\tilde{A}^1B_1 \leftarrow \tilde{X}^1A_1$ system that has led to

a revision in the position of the origin [50] we have recorded SVL emission spectra of $C^{79}Br^{81}Br$ and $C^{81}Br_2$ which probe the vibrational structure of the \tilde{X}^1A_1 state up to $\sim 7000 \text{ cm}^{-1}$ above the vibrationless level. These spectra reveal many previously unassigned levels, and a nearly complete set of vibrational parameters was determined from a Dunham expansion fit. The parameters are in good agreement with recent *ab initio* predictions. In the region between ~ 3600 and 5900 cm^{-1} , or between the singlet-triplet gap proposed by Hsu et al. [48] to that predicted by theory, we find that $\sim 90\%$ of the lines can be assigned to \tilde{X}^1A_1 levels within three standard deviations of our Dunham expansion fit. Higher resolution spectroscopic studies of the high energy region will be needed to gain further insight into the controversial singlet-triplet gap in CBr_2 ; however, the present work has set the stage for such experiments.

Acknowledgment

The National Science Foundation (Grant CHE-0353596) is gratefully acknowledged for support of this research.

Appendix A. Supplementary data

Supplementary data for this article are available on ScienceDirect (www.sciencedirect.com) and as part of the Ohio State University Molecular Spectroscopy Archives (http://msa.lib.ohio-state.edu/jmsa_hp.htm).

References

- [1] In: R.A. Moss, M. Jones, Jr., (Eds.), Carbenes, vol. I–II in Reactive Intermediates in Organic Chemistry Series, Wiley–Interscience, New York, 1973 (vol. I); 1975 (vol. II).
- [2] W. Kirmse, Carbene Chemistry, 2nd ed., Academic, New York, 1971.
- [3] J.C. Sciano, in: Handbook of Organic Photochemistry, vol. 2, CRC Press, Boca Raton, FL, 1989, Chapter 9.
- [4] M. Jones Jr., R.A. Moss, in: Reactive Chemical Intermediates, Wiley and Sons, Hoboken, New Jersey, 2004, Chapter 7.
- [5] G. Bertrand, in: Reactive Chemical Intermediates, Wiley and Sons, Hoboken, New Jersey, 2004, Chapter 8.
- [6] H. Tomioka, in: Reactive Chemical Intermediates, Wiley and Sons, Hoboken, New Jersey, 2004, Chapter 9.
- [7] K.K. Murray, D.G. Leopold, T.M. Miller, W.C. Lineberger, J. Chem. Phys. 89 (1988) 5442–5453.
- [8] M.K. Gilles, K.M. Ervin, J. Ho, W.C. Lineberger, J. Phys. Chem. 96 (1992) 1130–1141.
- [9] R.L. Schwartz, G.E. Davico, T.M. Ramond, W.C. Lineberger, J. Phys. Chem. A 103 (1999) 8213–8221.
- [10] C.-W. Chen, T.-C. Tsai, B.-C. Chang, Chem. Phys. Lett. 347 (2001) 73–78.
- [11] C.-W. Chen, T.-C. Tsai, B.-C. Chang, J. Mol. Spectrosc. 209 (2001) 254–258.
- [12] T.-C. Tsai, C.-W. Chen, B.-C. Chang, J. Chem. Phys. 115 (2001) 766–770.
- [13] H.-G. Yu, T. Lezana-Gonzalez, A.J. Marr, J.T. Muckerman, T.J. Sears, J. Chem. Phys. 115 (2001) 5433–5444.
- [14] C.-L. Lee, M.-L. Liu, B.-C. Chang, J. Chem. Phys. 117 (2002) 3263–3268.

- [15] C.-L. Lee, M.-L. Liu, B.-C. Chang, *Phys. Chem. Chem. Phys.* 5 (2003) 3859–3863.
- [16] M.-L. Liu, C.-L. Lee, A. Bezant, G. Tarczay, R.J. Clark, T.A. Miller, B.-C. Chang, *Phys. Chem. Chem. Phys.* 5 (2003) 1352–1358.
- [17] C.-S. Lin, Y.-E. Chen, B.-C. Chang, *J. Chem. Phys.* 121 (2004) 4164–4170.
- [18] W.-Z. Chang, H.-J. Hsu, B.-C. Chang, *Chem. Phys. Lett.* 413 (2005) 25–30.
- [19] G. Tarczay, T.A. Miller, G. Czako, A.G. Császár, *Phys. Chem. Chem. Phys.* 7 (2005) 2881–2893.
- [20] M. Deselnicu, C. Mukarakate, C. Tao, S.A. Reid, *J. Chem. Phys.* 124 (2006) 134302/1–134302/11.
- [21] C. Tao, C. Mukarakate, S.A. Reid, *J. Chem. Phys.* 124 (2006) 224314/1–224314/11.
- [22] C. Tao, M. Deselnicu, C. Mukarakate, S.A. Reid, *J. Chem. Phys.* 125 (2006) 094305/1–094305/9.
- [23] C.W. Bauschlicher Jr., H.F. Schaefer III, P.S. Bagus, *J. Am. Chem. Soc.* 99 (1977) 7106–7110.
- [24] P.H. Mueller, N.G. Rondan, K.N. Houk, J.F. Harrison, D. Hooper, B.H. Willen, J.F. Liebman, *J. Am. Chem. Soc.* 103 (1981) 5049–5052.
- [25] M.T. Nguyen, M.C. Kerins, A.F. Hegarty, N.J. Fitzpatrick, *Chem. Phys. Lett.* 117 (1985) 295–300.
- [26] E.A. Carter, W.A. Goddard III, *J. Phys. Chem.* 91 (1987) 4651–4652.
- [27] E.A. Carter, W.A. Goddard III, *J. Chem. Phys.* 88 (1988) 1752–1763.
- [28] S.K. Shin, W.A. Goddard III, J.L. Beauchamp, *J. Phys. Chem.* 94 (1990) 6963–6969.
- [29] S.J. Kim, T.P. Hamilton, H.F. Schaefer III, *J. Chem. Phys.* 94 (1991) 2063–2067.
- [30] G.L. Gutsev, T. Ziegler, *J. Phys. Chem.* 95 (1991) 7220–7228.
- [31] K.K. Irikura, W.A. Goddard III, J.L. Beauchamp, *J. Am. Chem. Soc.* 114 (1992) 48–51.
- [32] N. Russo, E. Sicilia, M. Toscano, *J. Chem. Phys.* 97 (1992) 5031–5036.
- [33] Z.-L. Cai, X.-G. Zhang, X.-Y. Wang, *Chem. Phys. Lett.* 210 (1993) 481–487.
- [34] A. Gobbi, G. Frenking, *J. Chem. Soc. Chem. Commun.* 14 (1993) 1162–1164.
- [35] V.M. Garcia, O. Castell, M. Reguero, R. Callol, *Mol. Phys.* 87 (1996) 1395–1404.
- [36] B.-S. Cheong, H.-G. Cho, *J. Phys. Chem. A* 101 (1997) 7901–7906.
- [37] S.S. Kumaran, M.-C. Su, K.P. Lim, J.V. Michael, S.J. Klippenstein, J. DiFelice, P.S. Mudipalli, J.H. Kiefer, D.A. Dixon, K.A. Peterson, *J. Phys. Chem. A* 101 (1997) 8653–8661.
- [38] D. Das, S.L. Whittenburg, *J. Mol. Struct. Theochem.* 492 (1999) 175–186.
- [39] M. Schwartz, P. Marshall, *J. Phys. Chem. A* 103 (1999) 7900–7906.
- [40] K. Sendt, G.B. Bacskay, *J. Chem. Phys.* 112 (2000) 2227–2238.
- [41] C.J. Barden, H.F. Schaefer III, *J. Chem. Phys.* 112 (2000) 6515–6516.
- [42] E.P.F. Lee, J.M. Dyke, T.G. Wright, *Chem. Phys. Lett.* 326 (2000) 143–150.
- [43] D.A. Dixon, K.A. Peterson, *J. Chem. Phys.* 115 (2001) 6327–6329.
- [44] M.L. McKee, J. Michl, *J. Phys. Chem. A* 106 (2002) 8495–8497.
- [45] J.M. Dyke, E.P.F. Lee, D.K.W. Mok, F.-T. Chau, *Chem. Phys. Chem.* 6 (2005) 2046–2059.
- [46] C.W. Bauschlicher Jr., *J. Am. Chem. Soc.* 102 (1980) 5492–5493.
- [47] R. Vargas, M. Galvan, A. Vela, *J. Phys. Chem. A* 102 (1998) 3134–3140.
- [48] H.-J. Hsu, W.-Z. Chang, B.-C. Chang, *Phys. Chem. Chem. Phys.* 7 (2005) 2468–2473.
- [49] C. Mukarakate, Y. Mishchenko, D. Brusse, C. Tao, S.A. Reid, *Phys. Chem. Chem. Phys.* 8 (2006) 4320–4326.
- [50] C. Tao, C. Mukarakate, D. Brusse, Y. Mishchenko, S.A. Reid, *J. Mol. Spectrosc.* 240 (2006) 139–140.
- [51] L. Andrews, *J. Chem. Phys.* 48 (1968) 979–982.
- [52] L. Andrews, T.G. Carver, *J. Chem. Phys.* 49 (1968) 896–902.
- [53] V.E. Bondybey, J.H. English, *J. Mol. Spectrosc.* 79 (1980) 416–423.
- [54] S.K. Zhou, M.S. Zhan, J.L. Shi, C.X. Wang, *Chem. Phys. Lett.* 166 (1990) 547–550.
- [55] S. Xu, M.D. Harmony, *J. Phys. Chem.* 97 (1993) 7465–7470.
- [56] NIST Atomic Spectra Database, V. 3.0 <<http://physics.nist.gov/PhysRefData/ASD>>.
- [57] S.A. Drake, J.M. Standard, R.W. Quandt, *J. Phys. Chem. A* 106 (2002) 1357–1364.
- [58] G. Herzberg, *Molecular Spectra and Molecular Structure III. Electronic Spectra of Polyatomic Molecules*, Van Nostrand, New York, 1966.